Journal of Oral Science, Vol. 60, No. 2, 304-315, 2018

Original

The effects of adding various ratios of zirconium oxide nanoparticles to poly(methyl methacrylate) on physical and mechanical properties

Gulfem Ergun[1)], Zeynep Sahin[2)], and Ayse Seda Ataol[2)]

[1)]Department of Prosthodontics, Faculty of Dentistry, Gazi University, Ankara, Turkey
[2)]Department of Prosthodontics, Faculty of Dentistry, Mersin University, Mersin, Turkey

(Received March 31, 2017; Accepted October 3, 2017)

Abstract: The aim of the present study is to evaluate the transverse strength, modulus of elasticity, surface roughness, hardness, and water sorption/solubility of nanoparticle zirconium oxide (nano-ZrO_2) added to heat-cured poly(methyl methacrylate) (PMMA) after thermocycling. The specimens were divided into four groups according to the ratio of nano-ZrO_2 addition to heat-cured PMMA; group 1: 5% nano-ZrO_2; group 2: 10% nano-ZrO_2; group 3: 20% nano-ZrO_2, and group 4 (control): PMMA without nano-ZrO_2. A statistically significant decrease in transverse strength was observed by all additional rates of nano-ZrO_2 compared with group 4 (control; $P < 0.025$). When hardness results were evaluated, groups 1 and 2 showed statistically higher values compared with groups 3 and 4 ($P < 0.025$). The surface roughness of group 3 was statistically higher than the other groups ($P < 0.025$), but it was within the clinically acceptable limits. As the nano-ZrO_2 addition rate increased, water sorption/solubility values of the specimens also increased. Although nano-ZrO_2 addition had an adverse effect on some mechanical and physical properties of heat-cured PMMA, it increased hardness values, implying that the addition of nano-ZrO_2 would contribute positively to some mechanical properties of PMMA denture base material when nano-ZrO_2 was homogeneously distributed in PMMA.

Correspondence to Dr. Gulfem Ergun, Department of Prosthodontics, Faculty of Dentistry, Gazi University, Biskek Street, Number:4, 06510 Emek, Ankara, Turkey
Fax: +90-3243610037 E-mail: ergungulfem@yahoo.com

Color figures can be viewed in the online issue at J-STAGE.
doi.org/10.2334/josnusd.17-0206
DN/JST.JSTAGE/josnusd/17-0206

Keywords: denture base material; zirconium oxide nanoparticles; physical properties; mechanical properties.

Introduction

Poly(methyl methacrylate) (PMMA) acrylic resin is often preferred as a denture base material due to its low cost, good adaptation, ease of application, and usage in tooth- or implant-supported removable/complete prostheses and orthodontic appliances (1-4). Clinically, improving the mechanical and physical properties of PMMA may be useful in points where masticatory forces are relatively high, such as distal extensions opposing natural teeth, single complete dentures, overdentures, and implant-supported complete dentures (3). This requirement is very important, especially in elderly patients, to eliminate situations such as denture fracture. Moreover, improving the mechanical and physical properties of PMMA may help elderly patients, who may be impaired or have difficulty adapting to a new denture, increase the lifespan of their prosthesis (5).

Various methods have been attempted to increase the strength of acrylic denture base and decrease the risk of denture fracture (6,7). Studies show that administering an appropriate additive to PMMA can improve the properties of polymers (1,4,6,8,9). Using high-strength resins or adding metal wire, glass fibers, barium titanate, silicon dioxide, titanium dioxide, zinc oxide, or hydroxyapatite are techniques used to reinforce PMMA (1,4,9). However, there are disadvantages to using these alternatives. For example, metal wires present poor adhesion with resin. Metal plates are expensive and prone to corrosion (10). Moreover, fibers cause tissue irritation (6).

Table 1 Tested materials used in the study

Material	Material content and properties	Lot no.	Manufacturer
Meliodent (heat-cured acrylic resin)	Powder: PMMA Liquid: MMA, dimethacrylate Mixing ratio: 35 g powder/14 mL liquid	RO10022	Heraeus Kulzer GmbH, Hanau, Germany
Stabilized zirconium oxide with yttrium	Form: Tetragonal (3% mole yttrium) Average particle dimension: ≤100 nm Specific surface area: 10-25 m^2/g	MKBV9830V	Sigma-Aldrich, St. Louis, MO, USA
ACS reagent	Toluene $-C_6H_5CH_3$ (≥99.7)	SZBF0090V	Sigma-Aldrich
APTES	3-Aminopropyltriethoxysilane (99%)	SHBG1799V	Sigma-Aldrich

Zirconium oxide (ZrO_2) is a metal oxide that possesses several advantages such as good mechanical strength, fracture toughness, hardness, wear and chemical resistance, and good thermal stability, thus making it beneficial for use in dental materials such as denture base reinforcement (4,8,11,12). ZrO_2 is a polymorphic material, is available in three stable phases: monoclinic, tetragonal, and cubic. The properties of ZrO_2 differ according to the phase types (13). The tetragonal phase is a catalytic phase, and it is a mechanically interesting phase compared with the other phases. Tetragonal phase ZrO_2 can be stabilized at room temperature with divalent and trivalent cationic species such as magnesium (Mg^{2+}), calcium (Ca^{2+}), and yttrium (Y^{3+}).

Nanotechnology has recently been used in the prosthodontic field for material enhancement purposes (9,12), which has been emphasized in the study of nanomaterials for improving the mechanical properties of PMMA. Nanofillers such as nanoclays, nanotubes, nanofibers, and nanoparticles are the current alternatives for improving the mechanical properties of PMMA (2). The effect of nanoparticles on the mechanical properties of PMMA depends on several factors including polymer-particle interface, particle size, fabrication method, and particle dispersion in the PMMA matrix (11,12). One of the most common nanoparticle fillers in use is ZrO_2. This bioceramic filler has high flexural strength and fracture toughness due to transformation toughening (7). Incorporating ZrO_2 into PMMA has been suggested to improve PMMA properties (4,12).

Recently, there have been many studies on the effect of ZrO_2 nanoparticle (nano-ZrO_2) addition as a filler to acrylic resin (14-16). The properties of the polymer-nanoparticle depend on the type of incorporating nanoparticles, their size and shape, as well as the concentration and interaction with the polymer matrix (16). Crystalline metal oxide nanoparticles aggregate in the organic media and are difficult to disperse homogeneously. Nanoparticle aggregates disrupt the mechanical properties and reduce the optic properties of polymer-based material. Good adhesion and dispersion homogeneity of nano-ZrO_2 with the resin matrix and the small nanoparticle size improve the transverse strength of PMMA (12,17). Therefore, organic solvents or monomer (silane coupling agent) could be used to disperse nanoparticles in the matrix (2,18).

The hardness of acrylic resins, which defines the ease of finishing a material and its resistance to wearing during cleaning, can be influenced by reinforcement materials (6) in addition to surface roughness. The roughness of PMMA is important as surface irregularities increase microorganism accumulation on the denture (19) and have undesired effects such as discoloration of the prosthesis. Moreover, water sorption and solubility are not favorable characteristics for denture base materials (20,21).

There are limited data available regarding the efficacy of nano-ZrO_2 on the mechanical and physical properties of heat-cured PMMA. This study aimed to evaluate the effect of tetragonal nano-ZrO_2 addition at three different concentrations (5%, 10%, and 20%) on the transverse strength, modulus of elasticity, microhardness, surface roughness, water sorption, and solubility of heat-cured PMMA base materials after aging by thermocycling.

Materials and Methods

The properties and contents of the test materials used in this study are shown in Table 1.

Chemical modification of nano-ZrO_2

In the present study, we used a silane coupling agent to double bond onto the surface of nano-ZrO_2 and distribution of nano-ZrO_2 fillers in the PMMA matrix. Moreover, we used 3-aminopropyltriethoxysilane (APTES) as a silane coupling agent to double bond onto the surface of nano-ZrO_2 and distribution nano-ZrO_2 fillers in the PMMA matrix. Toluene was used as an organic solvent. 1 mL APTES was diluted with 99 mL toluene to prepare the solution with 1% volume. The nano-ZrO_2 powder was mixed with this prepared solution in a magnetic

stirrer for 24 h and sieved. Each mixture process used 2 g of nano-ZrO_2 powder. The mixture was kept for 5 min in toluene and 10 min in the ultrasonic mixer. Fourier transform infrared spectroscopy (FTIR, Nicolet iS5, Thermo Scientific, Madison, WI, USA) analyses were performed to determine whether functional groups of silane coupling agent were attached to the nano-ZrO_2 by analyzing the characteristic vibrations of each functional group. Spectrum of the modified tetragonal nano-ZrO_2 was scanned over a 400-4,000 cm^{-1} wavenumber range.

Steel die was milled from a metal blank according to the dimension of each test specimen. The mold was filled with modeling wax and invested in a conventional dental flask. Heat-cured acrylic resin specimens were prepared after the dewaxing procedure.

For the test specimens of group 4 (control), resin powder of denture base material was mixed with monomer in a ratio of 23.4 g/10 mL according to the manufacturer's recommendation in each test. Tetragonal form of nano-ZrO_2 was used as the filler for fabricating the test specimens. The nano-ZrO_2 and heat-cured PMMA powder were pre-weighed to ensure a filler concentration of 5%, 10%, and 20% by weight according to the recommended powder/liquid ratio by the manufacturer. For example, the nano-ZrO_2 + heat-cured PMMA powder ratio for 1.5 mL liquid is as follows: Group 1: 0.1755 g nano-ZrO_2 + 3.3345 g heat-cured PMMA powder/1.5 mL liquid, Group 2: 0.351 g nano-ZrO_2 + 3.159 g heat-cured PMMA powder/1.5 mL liquid, Group 3: 0.702 g nano-ZrO_2 + 2.808 g heat-cured PMMA powder/1.5 mL liquid.

Resin powder of heat-cured PMMA was mixed and manipulated with monomer. Immediately thereafter, nano-ZrO_2 modified with silane coupling agent was added to the mixture. The ratio of the materials was determined according to the mixture proportion mentioned above for each test group. Next, they were manually mixed by spatulation until a homogeneous appearance was achieved. Thus, the test specimens were obtained.

Then, the test group specimens were cured with heat after dewaxing. Four tests were performed, and each test contained eight main subgroups. There were 80 specimens in each test (n = 10), consisting of a total of 320 specimens. Before each testing method, the specimens were initially polished by wet grinding with SiC papers (400, 600, and 800 grit). All specimens were stored in distilled water at 37°C (50 ± 2) h. Half of the test specimens were exposed to thermocycling (TC+) (SD Mechatronik Thermocycler, Julabo GmbH, FT 200, Seelbach, Germany) between 5°C and 55°C for 10,000 cycles with a 60 s dwell time and 6-s transfer time. The other half were stored in distilled water at 37°C in an incubator (TC−) (D-3162, Köttermann GmbH & Co. KG Labortechnik, Uetze, Germany) while the TC+ specimens were in the thermocycler.

Transverse strength and modulus of elasticity

The test specimens for transverse strength and modulus of elasticity were prepared according to the international standard no. ISO 20795-1 (22). Test specimens were prepared in the dimensions of 64 × 10 × 3.3 mm. The three-point bending test was applied for transverse strength and modulus of elasticity, and force was applied until failure occurred with a universal testing machine (Lloyd Instruments, Fareham, UK) in the midpoint of the specimens. The speed of the device was determined according to the ISO 20795-1 (5 ± 1 mm/min). The formulas used to calculate the transverse strength and modulus of elasticity are as follows:

$S = 3FI / 2bh^2$ and $E = FI^3 / 4bh^3d$

(S = transverse strength (MPa), E = modulus of elasticity (MPa), F = maximum load at the moment of fracture (N), l = distance between the supports, b = specimen width, and h = specimen thickness, mm).

Microhardness test

Surface hardness was determined using Digital Display Vickers Microhardness Tester (HMV, Shimadzu, Kyoto, Japan). The test specimens were fabricated using the dimensions of 30 × 30 × 2.5 mm. The microhardness tester was adjusted to a load of 0.49 N for 5 s indentation time. Three indentations were equally placed over a specimen and were no closer than 1 mm to the adjacent indentations or to the margin of the specimens. The diagonal length of the indentations was measured on a microscopic scale, and surface microhardness was calculated automatically.

Surface roughness

Surface roughness (Ra) of the tested specimens, which were prepared as disk shaped with a diameter of 10 mm and thickness of 2 mm, was recorded with a profilometer device (Perthometer M2, Mahr, Göttingen, Germany). The device had a diamond stylus that moved in contact with the surface. Three measurements were made for each specimen at three points across each specimen surface, which was divided into three equal parts. Each line was scanned with a constant force of 0.7 mN on the diamond stylus. The mean of these three readings was recorded as the surface roughness value.

Water sorption and solubility

The disk-shaped specimens (diameter of 50 ± 1 mm and

thickness of 2 ± 0.05 mm) were prepared and placed in a desiccator (ILDAM Ltd., Ankara, Turkey) with newly dried silica gel (Sigma-Aldrich, Sternheim, Germany) at 37 ± 1°C for 24 h. The drying cycle was repeated every day at the same time until the specimens reached a constant mass (M1). They were placed in distilled water for 7 days at 37 ± 1°C, removed, and weighed again (M2). After this process, they were placed in the desiccator again until they reach a constant mass as stated previously. This renewed mass was recorded as M3. Water sorption and solubility were calculated using the following formula:

W_S (μg/mm^3) = M2 (μg) – M3 (μg) / V (mm^3)

W_{SL} (μg/mm^3) = M1 (μg) – M3 (μg) / V (mm^3)

Scanning electron microscope (SEM) examination

Two specimens were randomly selected from the flexural strength test groups and coated with a gold/palladium film layer using 10^{-1} hPa/Pa combustion room pressure and a current of 10 mA for 180 s in the gold/palladium coating unit (Sputter Coater SC7620, Polaron, VG Microtech, Uckfield, UK). SEM (JSM-6060 LV, JEOL, Tokyo, Japan) images were obtained with magnifications of ×50, ×100, ×500, ×1,000, and ×1,500. The specimens were evaluated with SEM not only to examine the surface for porosity and other defects but also to observe the incorporation of fillers in polymer matrix.

X-ray diffractometer (XRD) analysis

Crystalline phase and structure identification of nano-ZrO_2 were performed using XRD (SmartLab, Rigaku, Tokyo, Japan). The XRD patterns were measured in the 8-80° 2θ range at room temperature, and 5°/min of scanning speed was used. The average crystallite size of nano-ZrO_2 was estimated using the Scherrer formula (11):

$D = 0.9\lambda / B\cos\theta$

In the above-mentioned formula, D is the average crystallite size, λ is the X-ray wavelength (Cu-K_α radiation; 0.154056 nm), B is the full width at half maximum (FWHM) width of the diffraction peak, and θ is the corresponding diffraction angle of the diffraction peak.

Statistical analysis

Calculated values for the test parameters were statistically analyzed using IBM SPSS Statistics version 17.0 software (IBM Corporation, Armonk, NY, USA). Furthermore, the Kolmogorov-Smirnov test was used to determine whether the distributions of continuous variables were normal, and the Levene test was used to evaluate the homogeneity of variance. Data were shown as median. Also, the Mann-Whitney *U* test assessed whether the differences between groups with and without thermocycle were statistically significant. According to the Bonferroni correction, $P < 0.0125$ was considered statistically significant. Kruskal-Wallis was applied for comparisons among more than two independent groups. According to the Bonferroni correction, $P < 0.025$ was considered statistically significant. Conover multiple comparison test was used when the *P* value from the Kruskal-Wallis test was statistically significant to determine which group was different. In the current study, the Bonferroni correction was applied to control for Type I error in all possible multiple comparisons.

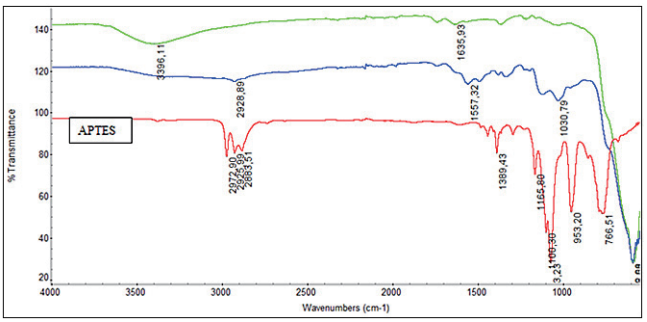

Fig. 1 FTIR spectrum (red: silane coupling agent "APTES", blue: tetragonal nano-ZrO_2 modified with silane coupling agent, and green: tetragonal nano-ZrO_2).

Results

The FTIR test was applied to the nano-ZrO_2 specimens before and after silanization and silane coupling agent to evaluate the differences in the active groups. Three strong absorption bands were seen at wavenumbers of 3,396, 1,635, and 588 cm^{-1} in tetragonal nano-ZrO_2 (Fig. 1, green line). Two bands in 3,396 and 1,635 cm^{-1} resulted from the tension vibration of the hydroxyl groups on the nano-ZrO_2 surface. The absorption band in 588 cm^{-1} was due to the vibration of the Zr-O bond. Three new strong absorption peaks were seen at wavenumbers of 2,928, 1,557, and 1,030 cm^{-1} in the FTIR spectrum of modified nano-ZrO_2 with silane coupling agent (Fig. 1, blue line). These peaks, respectively, demonstrated the stress vibration of C-H bond, symmetrical bonding of -NH3+, and stress vibration of Si-O-Zr bond. Two new absorption bands, stress vibration of C-H bond in the range of 2,800-3,000 cm^{-1} and that of Si-O-Zr bond in the range of 800-1,200 cm^{-1}, showed that silane coupling agent was successfully bonded to nano-ZrO_2 (Fig. 1).

Groups 1, 2, and 3 showed statistically significantly lower transverse strength compared with group 4 (control; $P < 0.025$; Table 2). Groups 1 and 2 did not show statistically significant differences in transverse strength

Table 2 Transverse strength (MPa) results of the tested specimens

	TC−	TC+	*P* value†
Group 1	70.4 (64.7-75.9)[a,d]	67.3 (56.6-84.4)[a,d]	0.739
Group 2	50.0 (48.1-61.7)[b,e]	55.8 (49.8-60.0)[b,e]	0.579
Group 3	39.5 (37.5-43.9)[c,d,e]	40.7 (33.8-43.8)[c,d,e]	0.853
Group 4 (control)	96.2 (80.1-113.2)[a,b,c]	101.8 (94.5-106.2)[a,b,c]	0.579
P value‡	<0.001	<0.001	

The data are shown in median (interquartile range). †The comparisons among the groups according to the thermocycle, Mann-Whitney *U* test, the results were accepted as statistically significant for $P < 0.0125$ according to the Bonferroni correction. ‡The comparisons among all of the test groups, Kruskal-Wallis test, the results were accepted as statistically significant for $P < 0.025$ according to the Bonferroni correction. The same superscript letters indicate statistically significant differences between the stated groups; a: Group 1 vs 4 (control; $P < 0.025$), b: Group 2 vs 4 (control; $P < 0.025$), c: Group 3 vs 4 (control; $P < 0.025$), d: Group 1 vs 3 ($P < 0.025$), e: Group 2 vs 3 ($P < 0.025$).

Table 3 Modulus of elasticity values of the tested specimens

	TC−	TC+	*P* value†
Group 1	5121.6 (4704.4-5923.7)	5539.5 (4908.6-5927.4)	0.481
Group 2	5257.1 (4467.1-5799.7)	5392.7 (4331.0-5822.5)	0.684
Group 3	4793.8 (4385.4-5271.4)	4399.4 (3789.2-5201.4)	0.353
Group 4 (control)	5483.9 (4802.6-6245.3)	5628.4 (5109.6-6248.1)	0.529
P value‡	0.323	0.030	

The data are shown in median (interquartile range). †The comparisons among the groups according to the thermocycle, Mann-Whitney *U* test. The results were accepted as statistically significant for $P < 0.0125$ according to the Bonferroni correction. ‡The comparisons among all of the test groups, Kruskal-Wallis test, the results were accepted as statistically significant for $P < 0.025$ according to the Bonferroni correction.

Table 4 Microhardness values of the tested specimens

	TC−	TC+	*P* value†
Group 1	36.8 (33.4-42.8)[a,c]	35.2 (32.6-39.1)[a,c,e]	0.529
Group 2	36.2 (34.4-37.9)[b,d]	31.3 (30.0-36.5)[d,e]	0.029
Group 3	33.3 (31.5-35.1)[c,d]	28.1 (24.2-30.9)[c,d]	0.009
Group 4 (control)	32.6 (30.8-34.8)[a,b]	31.6 (29.3-32.9)[a]	0.353
P value‡	<0.001	0.003	

The data are shown in median (interquartile range). †The comparisons among the groups according to the thermocycle, Mann-Whitney *U* test, the results were accepted as statistically significant for $P < 0.0125$ according to the Bonferroni correction. ‡The comparisons among all of the test groups, Kruskal-Wallis test, the results were accepted as statistically significant for $P < 0.025$ according to the Bonferroni correction. The same superscript letters indicate statistically significant differences between the stated groups: a: Group 1 vs 4 (control; $P < 0.025$), b: Group 2 vs 4 (control; $P < 0.025$), c: Group 1 vs 3 ($P < 0.025$), d: Group 2 vs 3 ($P < 0.025$), e: Group 1 vs 2 ($P < 0.025$).

($P > 0.025$), but the increase in the addition ratio of nano-ZrO_2 resulted in decreased transverse strength values in group 2. Group 3 showed statistically significantly lower transverse strength compared with groups 1 and 2 ($P < 0.025$), revealing that, as the ratio of nano-ZrO_2 increased, the transverse strength of heat-cured PMMA decreased. Moreover, thermocycling had no statistically significant effect on flexural strength in any of the tested groups ($P > 0.0125$).

There were no statistically significant differences among the groups tested in terms of modulus of elasticity ($P > 0.025$); however, there was a decrease in the nano-ZrO_2 addition groups compared with group 4 (control; Table 3). Moreover, thermocycling had no statistically significant effect on the modulus of elasticity of any of the test groups compared with the TC− groups ($P > 0.0125$).

In the TC− groups, nano-ZrO_2 addition increased the surface hardness of all test specimens compared with that in group 4 (control; Table 4). The hardness increase in group 2 was statistically significant compared with that in group 4 (control; $P < 0.025$; TC−). Group 1 revealed statistically significantly higher surface hardness compared with that in groups 3 and 4 ($P < 0.025$; TC−, TC+). Similarly, group 2 demonstrated statistically significantly higher surface hardness compared with group 3 ($P < 0.025$; TC−, TC+). The highest surface hardness value (36.8) was obtained in group 1 (TC−).

Table 5 Surface roughness results of the tested specimens

	TC−	TC+	*P* value†
Group 1	0.19 (0.16-0.30)^{c}	0.21 (0.16-0.25)^{c}	0.971
Group 2	0.40 (0.18-0.49)^{a,d}	0.24 (0.18-0.45)^{d}	0.393
Group 3	1.06 (0.72-1.16)^{b,c,d}	0.94 (0.71-1.30)^{b,c,d}	0.912
Group 4 (control)	0.14 (0.13-0.17)^{a,b}	0.16 (0.15-0.26)^{b}	0.190
P value‡	<0.001	<0.001	

The data are shown in median (interquartile range). †The comparisons among the groups according to the thermocycle, Mann-Whitney *U* test, the results were accepted as statistically significant for $P < 0.0125$ according to the Bonferroni correction. ‡The comparisons among all of the test groups, Kruskal-Wallis test, the results were accepted as statistically significant for $P < 0.025$ according to the Bonferroni correction. The same superscript letters indicate statistically significant differences between the stated groups; a: Group 2 vs 4 (control; $P < 0.025$), b: Group 3 vs 4 (control; $P < 0.025$), c: Group 1 vs 3 ($P < 0.025$), d: Group 2 vs 3 ($P < 0.025$).

Table 6 Water sorption (μg/mm^3) values of the tested specimens

	TC−	TC+	*P* value†
Group 1	7.5 (6.2-8.1)^{a,d}	7.1 (6.1-8.1)^{d,f}	0.739
Group 2	9.2 (8.3-9.7)^{b,e}	8.9 (8.4-9.8)^{b,e,f}	0.971
Group 3	14.4 (12.9-16.2)^{c,d,e}	17.1 (14.5-18.8)^{c,d,e}	0.105
Group 4 (control)	6.1 (5.9-6.4)^{a,b,c}	6.3 (6.0-6.6)^{b,c}	0.218
P value‡	<0.001	<0.001	

The data are shown in median (interquartile range). †The comparisons among the groups according to the thermocycle, Mann-Whitney *U* test, the results were accepted as statistically significant for $P < 0.0125$ according to the Bonferroni correction. ‡The comparisons among all of the test groups, Kruskal-Wallis test, the results were accepted as statistically significant for $P < 0.025$ according to the Bonferroni correction. The same superscript letters indicate statistically significant differences between the stated groups; a: Group 1 vs 4 (control; $P < 0.025$), b: Group 2 vs 4 (control; $P < 0.025$), c: Group 3 vs 4 (control; $P < 0.025$), d: Group 1 vs 3 ($P < 0.025$), e: Group 2 vs 3 ($P < 0.025$), f: Group 1 vs 2 ($P < 0.025$).

Table 7 Water solubility (μg/mm^3) values of the tested specimens

	TC−	TC+	*P* value†
Group 1	0.92 (0.32-1.02)^{c,d}	0.51 (0.29-0.79)^{d}	0.165
Group 2	1.87 (1.29-2.30)^{a,c}	1.02 (0.54-1.25)^{a,e}	<0.001
Group 3	3.22 (2.20-4.67)^{b,d}	3.34 (2.55-5.50)^{b,d,e}	0.684
Group 4 (control)	0.35 (0.12-0.60)^{a,b}	0.19 (0.05-0.66)^{a,b}	0.796
P value‡	<0.001	<0.001	

The data are shown in median (interquartile range). †The comparisons among the groups according to the thermocycle, Mann-Whitney *U* test, the results were accepted as statistically significant for $P < 0.0125$ according to the Bonferroni correction. ‡The comparisons among the test groups, Kruskal-Wallis test, the results were accepted as statistically significant for $P < 0.025$ according to the Bonferroni correction. The same superscript letters indicate statistically significant differences between the stated groups; a: Group 2 vs 4 (control; $P < 0.025$), b: Group 3 vs 4 (control; $P < 0.025$), c: Group 1 vs 2 ($P < 0.025$), d: Group 1 vs 3 ($P < 0.025$), e: Group 2 vs 3 ($P < 0.025$).

Group 1 (TC+) revealed statistically significantly higher surface hardness than did group 2 ($P = 0.02$). The test specimens in group 3 showed significantly decreased surface hardness after thermocycling ($P = 0.009$), and the other test groups had nonsignificantly lower surface hardness compared with that in the TC− groups ($P > 0.0125$).

The nano-ZrO_2 addition increased the surface roughness of all test specimens compared with that in group 4 (control; TC−, TC+; Table 5). In particular, group 3 indicated statistically significantly higher surface roughness values compared with groups 1, 2, and 4 ($P < 0.025$; TC−, TC+). Group 3 (TC−) revealed the highest surface roughness value (Ra = 1.06) compared with the other test groups. Moreover, thermocycling showed no statistically significant effect on the surface roughness of the test specimens among the test groups ($P > 0.0125$; TC−, TC+).

Water sorption values increased parallel to the increase in nano-ZrO_2 added to PMMA (Table 6). Moreover, thermocycling had no statistically significant effect on the water sorption of all test specimens ($P > 0.0125$). Group 3 exhibited the highest water sorption values among the test groups (17.1 μg/mm^3).

The increase in nano-ZrO_2 addition increased the water solubility value (Table 7). Groups 2 and 3 displayed

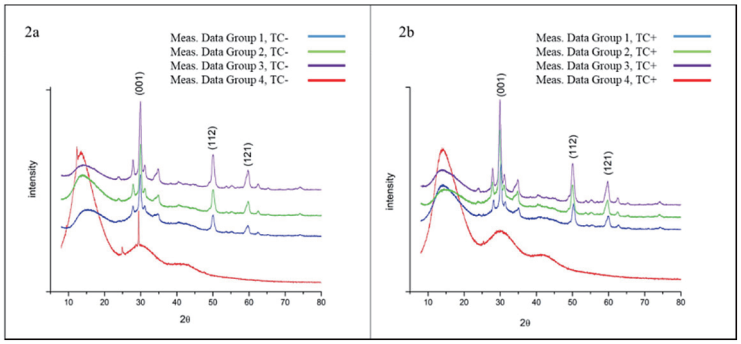

Fig. 2 XRD analyses of the tested specimens. a. water storage, TC−; b. thermocycle, TC+.

Table 8 The average crystal size of nano-ZrO_2 according to XRD analyses

	The average crystal of nano-ZrO_2 (water storage) (TC−)	The average crystal of nano-ZrO_2 (thermocycle) (TC+)
Group 1	15.429 nm	14.926 nm
Group 2	14.382 nm	15.121 nm
Group 3	15.332 nm	15.321 nm

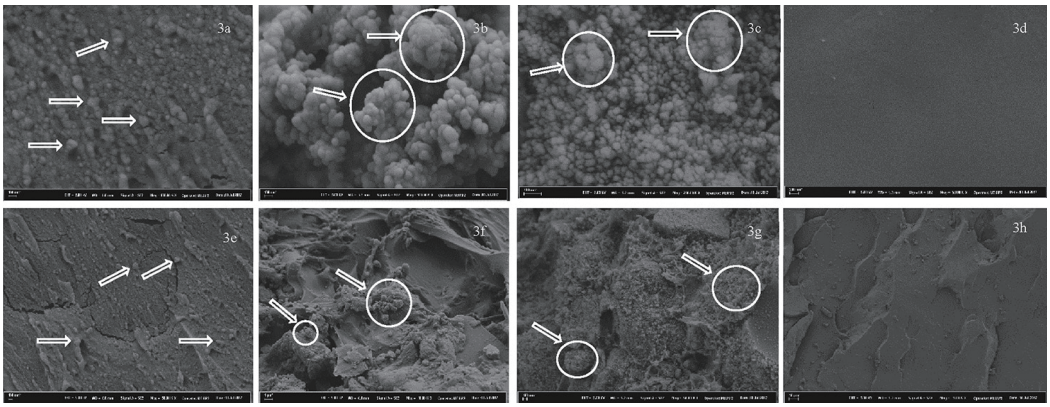

Fig. 3 SEM images of tested specimens. a, e: Group 1, homogeneous dispersion of nano-ZrO_2 (arrows). b, f: Group 2, accumulation of nano-ZrO_2 (arrows). c, g: Group 3, accumulation of nano-ZrO_2 (arrows). d, h: Group 4 (control).

statistically significantly higher water solubility than group 4 (control; $P < 0.025$), and group 3 had statistically higher water solubility than group 1 ($P < 0.025$). Only specimens in group 2 demonstrated a significant decrease in water solubility after thermocycling ($P < 0.0125$).

XRD analysis was used to examine the crystal structure of nanoparticles added into heat-cured PMMA base materials. Figure 2a and b shows XRD patterns of all the tested groups. XRD spectra demonstrated characteristic peaks for ZrO_2 (DB card number: ICCD 00-050-1089). Nano-ZrO_2 had sharper and narrower peaks at around 2θ = 30.0°, 50.08°, and 59.05°, which were assigned to reflections from planes (001), (112), and (121), respectively, corresponding to tetragonal nano-ZrO_2. The diffraction patterns of all of the tested heat-cured PMMA (groups 1, 2, and 3) represented the same three bands that were not observed in group 4 (control; pure heat-cured PMMA). Table 8 contains the average crystallite size of nano-ZrO_2 according to the Scherrer formula.

$D = 0.9\lambda / B\cos\theta_B$

Moreover, the thermocycling procedure did not significantly affect the crystallite size of nano-ZrO_2 (Table 8).

The homogeneity of the nanoparticle filler mixture was examined by SEM. Examples of the results are seen in Fig. 3. The nanoparticle fillers were distributed better in group 1 than in groups 2 and 3 (Fig. 3a-c). The SEM images of groups 2 and 3 indicated that nano-ZrO_2 was not distributed homogeneously and displayed accumulation in the heat-cured PMMA matrix (Fig. 3b, c). Fractured surfaces were also observed by SEM (Fig. 3e-h). Nano-ZrO_2 dispersion in group 1 (Fig. 3e) was relatively homogeneous compared with that in groups 2

and 3 (Fig. 3f, g). Groups 2 and 3 (Fig. 3f, g) indicated that the increased nano-ZrO_2 percentage resulted in an increased accumulation of nano-ZrO_2.

Discussion

Nano-ZrO_2 is expected to improve the mechanical properties in PMMA. In contrast, the addition of various ratios (5%, 10%, and 20%) of nano-ZrO_2 to heat-cured PMMA decreased the transverse strength values compared with those for group 4 (control) in our study. The highest flexural strength was 101.8 MPa obtained from group 4 (control; TC+). However, group 3 revealed the lowest flexural strength (39.5 MPa) among the tested groups. The transverse strength of the test specimens was decreased with the increased nano-ZrO_2 filler rate. The increased nanoparticle filler content caused defects that weakened the material; therefore, the increased filling rate did not lead to increased mechanical strength (3). The transverse strength should not be <65 MPa for heat-cured acrylic resin according to ISO 20795-1 (22). In the present study, the transverse strength of groups 1 and 4 was not lower than 65 MPa, which was compatible with the reference value, but the values in groups 2 and 3 were lower than 65 MPa.

Our results differed from most of the previous studies (4,14). For example, Ayad et al. (14) reported that 5% and 15% of ZrO_2 addition significantly increased the transverse strength of acrylic resins. Moreover, Asopa et al. (3) indicated that the addition of ZrO_2 at concentrations of 10% resulted in increased flexural strength. The mechanical properties of the resins were affected by the filler type and size. ZrO_2 particle size was not specified in the study of Ayad et al. (14). Moreover, ZrO_2 powder, which was not a nanoparticle with an average particle size of 5,000-10,000 nm, was used as a filler in the study conducted by Asopa et al. (3). In our study, when added to heat-cured PMMA, the use of nano-ZrO_2 as filler particles of ≤100 nm could not fill the matrix homogeneously; these differences may be caused by the difference in the percentage of ZrO_2, filler size, and type of acrylic resin used. Furthermore, the differences may be related with the nonhomogenous distribution of nano-ZrO_2 within the PMMA matrix (Fig. 3a-c, e-g).

The ratio of the nanoparticle used for reinforcement should be at a rate that can be distributed in the matrix resin without interrupting the continuity of the matrix. In their study, Alhareb and Ahmad (1) reported that well-dispersed particles enhanced crack propagation paths. Moreover, Gad et al. (12) stated that the incorporation of nano-ZrO_2 resulted in a significant increase in transverse strength values, which was associated with good distribution of the nano size particles that fill the spaces between polymeric chains (12). However, Ihab and Moudhaffar (23) revealed that increasing the percentage of modified nano-ZrO_2 to 7 wt% lowered the transverse strength of PMMA due to the agglomeration of nano-ZrO_2. In our study, SEM evaluation of the fracture surface of the specimens (Fig. 3f, g) showed nonhomogeneous dispersion within the resin matrix. Nanoparticles have a strong tendency to aggregate due to the high specific surface area, surface energy, and chemical activity. This clustering, as seen in the current study, resulted in a decreased reinforcement effect on the PMMA matrix. The increased accumulation of nano-ZrO_2 (especially in groups 2 and 3; Fig. 3f, g) may be related to the decreased transverse strength compared with that in the control groups.

Methacryloxypropyltrimethoxysilane, 3-glycidoxypropyltrimethoxysilane, and APTES are the most frequently used silane coupling agents for various purposes. These agents can be adsorbed on nanoparticles for fabricating functionalized silica nanoparticles (18,24). ZrO_2 nanoparticles and APTES attach via the condensation of a trialkoxy group with the hydroxyl group of nano-ZrO_2 (24). In previous studies, ZrO_2 nanocrystal dispersion was examined with organic dissolvers such as toluene, pyridine, ethane nitrile, acetone, and isopropyl (18,24). Luo et al. (24) reported that APTES and IPTES were efficient for the dispersion of ZrO_2 nanocrystals in pyridine and toluene. In the present study, APTES, which is the most commonly applied silane coupling agent, is used to functionalize nano-ZrO_2 with toluene as an organic dissolver. Moreover, the attachment of the functional groups of silane coupling agents was confirmed by FTIR analysis by analyzing the characteristic vibrations of the functional groups (Fig. 1). However, Zhang et al. (15) indicated that another way to control the filler dispersion to the PMMA matrix was to manipulate the nano-ZrO_2/PMMA nanocomposite preparation procedure. They reported that mechanical attrition such as bead ball milling and ultrasonication could be used to resist nanoparticle clustering during the modification procedure. Although we used an ultrasonic mixer during silanization of nano-ZrO_2, only mechanically mixing the modified nano-ZrO_2 and PMMA powder may be the cause of nano-ZrO_2 clustering and decreased strength values.

The decreased mechanical properties may have been caused by the effect of the tetragonal-to-monoclinic phase transformation of ZrO_2. ZrO_2 volume expansion due to the phase transformation may cause microcracks on the APTES-coated surface of nano-ZrO_2 (25). In the current study, the flexural strength test specimens

were stored in distilled water prior to the three-point bending test for 50 ± 2 h; these microcracks absorbed the water during the procedure. Water absorption into the polymer network negatively affects some physical and mechanical properties of PMMA and can lead to a decrease in flexural strength (3,14,20). The decrease in flexural strength of groups 1, 2, and 3 may be related with the increased water sorption of the specimens before the flexural strength test.

Relatively low modulus of elasticity makes PMMA more prone to failure in the mouth (26). The modulus of elasticity should be at least 2,000 MPa for heat acrylic resin according to ISO 20795-1 (22). In our study, although the increase in the filler ratio of nano-ZrO_2 decreased the modulus of elasticity, the elasticity modulus values of the tested specimens were higher than 2,000 MPa. Nano-ZrO_2 fillers with different ratios do not act as good reinforcing fillers in heat-cured PMMA, making the structure more brittle.

Polymerized acrylic resin hardness is an important material property in terms of residual monomer content in the resin material (17) and resistance to wear (27). Moreover, hardness measurement has been used as an indirect method of evaluating polymerizing depth of resin-based materials (17). Moreover, hardness impacts the surface characteristics of PMMA indicating the ease of finishing a material (6). These days, nano-ZrO_2 is used to fabricate reinforced denture base materials with high hardness (17,28).

The results of the current study demonstrated a statistically significant increase in the hardness of groups 1 and 2 (water storage groups) compared with the other groups ($P < 0.01$). The highest hardness value was observed in group 1 (TC− 36.8, TC+ 35.2). As the amount of fillers increased, the nano-ZrO_2 surface remained clear, displaying poor adhesion to the matrix and clusters in the resin matrix (especially in group 3). SEM analysis showed homogenous dispersion of nanoparticles in group 1 compared with that in group 3 (Fig. 3a, c). Results of the current study revealed that heat-cured PMMA reinforcement in terms of hardness was obviously related to the filler amount presented in the resin matrix and the dispersion homogeneity.

Previous studies have mostly concluded that reinforcing acrylic resins with ceramic particles can provide some improvements in surface hardness (6,17); these findings are in agreement with the results for group 1 in the present study and are not in agreement with those for group 3 due to nonhomogeneous nanoparticle dispersion and low ionic interatomic bonding. Similarly, Asopa et al. (3) reported that 10% and 20% of nano-ZrO_2 addition to PMMA resulted in a significant increase in flexural strength but a decrease in surface hardness. Therefore, the weak interfacial bond between the nanofiller and resin matrix could be the reason there was no significant increase in hardness in the high ratio of nano-ZrO_2 addition groups in the present study (especially in group 3).

Although in a previous study (17), the nanofiller addition ratio (1.5%, 3%, 5%, and 7%) was lower than in our study, those authors reported a significant increase in hardness as the percentage of nano-ZrO_2 fillers increased, suggesting that this result was related to the high interfacial shear strength between the nanofiller and resin matrix as a result of cross-link formation or supramolecular bonding (17). In the present study, increased hardness in groups 1 and 2 could be related with the strength characteristics of nano-ZrO_2 (17). ZrO_2 has strong ionic interatomic bonding that provides desirable material characteristics such as hardness.

Surface irregularities increase microorganism accumulation on the denture surface (19,29). Therefore, the nanoparticle addition must enable the surface roughness to remain within acceptable clinical limits while improving the mechanical properties of the material.

According to ISO 20795-1, the critical Ra value that is clinically acceptable for acrylic resin is 0.2 μm (22). Bacterial colonization significantly increases if the surface roughness value is higher than 0.2 μm (30). The roughness results of the present study were higher than the threshold value for Ra (except in groups 1 and 4; Table 5). The increase in surface roughness of the test specimens was proportional to the concentration of nano-ZrO_2, and there was a slight increase in group 1. In agreement with the study by Ihab and Moudhaffar (23), our study found that the increased surface roughness values of group 1 (5%) were not statistically significant compared with those of group 4 (control; $P > 0.025$), and the increase was within the clinically acceptable limits (0.19 μm for TC− and 0.21 μm for TC+). Group 3 (TC−) displayed a significant increase in roughness, with the highest surface roughness value (1.06 μm), compared with the other test groups ($P < 0.001$), which is possibly due to the small size of the nano-ZrO_2 particles, which were well dispersed especially in group 1. Moreover, when nano-ZrO_2 was added to PMMA at a low rate (5%), only a few particles were exposed on the surface of the test specimens as mentioned in the study of Ihab and Moudhaffar (23). Aljafery and Mah (31) revealed that the surface roughness of modified PMMA with 2% ZrO_2-Al_2O_3 nanoparticles was significantly increased compared with that in group 4 (control). In agreement with the previous study (31), the increased surface rough-

ness along with the increased presence of nanofillers in the present study may be due to the different roughness of nanoparticles and acrylic denture base matrix or the different microstructural characteristics of the materials and the form of the particles.

The surface roughness of acrylic resin varies between 0.03 and 0.75 mm depending on the finishing and polishing technique utilized (30,32). In our study, the surface of the test specimens was standardized by wet grinding with SiC papers (400, 600, and 800 grit). The Ra values of the test specimens were between 0.14 and 1.06 without polishing. Ra value results for group 4 (control) in the present study were within the clinically acceptable Ra threshold values, suggesting that the increased Ra values within the nano-ZrO_2 addition groups was not related to the surface standardization procedure used in this study and may be due to the roughness differences between nano-ZrO_2 and acrylic denture base matrix or the differences in microstructural characteristics of the material, the form of the nano-ZrO_2, or the nonhomogeneous dispersion of nano-ZrO_2 especially in group 3.

It is known that PMMA is prone to absorb water over a period due to molecular polarity. Water absorbs into the material by a diffusion mechanism among the polymer chains and damages the bonding of the polymer network (33). Repeated sorption/desorption cycles cause microfractures in the PMMA matrix (21). Moreover, the solubility of the acrylic resins is a result of unreacted monomer and water-soluble additives leaching out into the oral fluids. Low solubility of denture base materials is desired due to the soft tissue reaction of the monomer (34).

The effect of different filler additions, such as glass fiber, Al_2O_3, and ZrO_2, on water sorption and solubility has been studied previously (3,14,33). It has been reported that Al_2O_3 nanoparticle polymers served as a site for the prevention of water absorption (35). The Al_2O_3-added groups exhibited significantly lower water sorption values compared with those in group 4 (control) due to the insolubility of Al_2O_3 nanoparticles in water. However, previous studies have indicated that the addition of nanoparticle fillers to improve the mechanical properties of PMMA increases the water sorption of acrylic resins (4,36,37). In particular, the increase in the nanoparticle filler ratio causes more water sorption because of more nanoparticle filler-matrix particle interface. The weak polymer chains allow water permeability into the matrix (4). For example, Asopa et al. (3) reported that water sorption of 10% and 20% nano-ZrO_2-added PMMA was found to increase but was within the limit of ADA Specification No. 12, which is similar to our results. They reported that the excessive increase in the value of water sorption may be related to the weak secondary bonds.

According to the ISO 20795-1 standard, 32 μg/mm^3 is the threshold value for water sorption, and 1.6 μg/mm^3 is the threshold value for water solubility of heat-cured acrylic resins (22). Group 4 (control) exhibited the lowest mean water sorption values of TC− 6.1 μg/mm^3 and TC+ 6.3 μg/mm^3, which were significantly lower than the other tested groups. The addition of nano-ZrO_2 in heat-cured PMMA increased the water sorption in all test groups, but the values were within clinically acceptable limits. The addition of 10% and 20% nano-ZrO_2 statistically significantly increased the water sorption compared with that in group 4 (control). The highest water sorption value was obtained in group 3 (TC− 14.4 μg/mm^3 and TC+ 17.1 μg/mm^3), which was not below the threshold value and was in agreement with the results of previous studies (3,14,37). Solubility test results showed that as the ratio of added nano-ZrO_2 increased, the solubility values increased concurrently. The water solubility values of the present study were generally within the clinically acceptable limits (except in group 3). However, group 3 exhibited the highest water solubility values (TC− 3.22 μg/mm^3 and TC+ 3.34 μg/mm^3). It is well known that porosity can occur among polymer chains during the polymerization process of acrylic resins. The increased porosity has been shown to simplify liquid transport into and out of polymer (35). By considering the results above, the main reason the highest water sorption and solubility values were obtained in group 3 may be related to the increased filler rate and the weak bond of nano-ZrO_2 to the heat-cured PMMA matrix.

We experienced difficulty in uniformly dispersing the nanoparticle fillers in the heat-cured PMMA matrix during the test specimen production. Therefore, it is important to investigate new applications to provide homogenous distribution and bonding of nano-ZrO_2 to heat-cured PMMA matrix. Further research is needed to examine the effects of nano-ZrO_2 addition on the mechanical and physical properties of heat-cured PMMA.

This report was presented as an oral presentation at 2017 FDI Annual World Dental Congress, August 29-September 1, 2017, Madrid, Spain (Publication number: FC089)

Acknowledgments

This work was supported by the Unit of Scientific Research Projects Fund of Gazi University, Ankara, Turkey (Grant number: 03/2015-12).

Conflict of interest
None declared.

References

1. Ahmed Omran A, Zainal Arifin A (2011) Effect of Al_2O_3/ZrO_2 reinforcement on the mechanical properties of PMMA denture base. J Reinf Plastic Comp 30, 86-93.
2. Kareem S, Moudhaffer M (2015) The effect of zirconium silicate nanopowder reinforcement on some mechanical and physical properties of heat cured poly (methyl methacrylate) denture base materials. J Baghdad Coll Dent 27, 37-43.
3. Asopa V, Suresh S, Khandelwal M, Sharma V, Asopa SS, Kaira LS (2015) A comparative evaluation of properties of zirconia reinforced high impact acrylic resin with that of high impact acrylic resin. Saudi J Dent Res 6, 146-151.
4. Maji P, Choudhary RB, Majhi M (2016) Structural, optical and dielectric properties of ZrO_2 reinforced polymeric nanocomposite films of polymethylmethacrylate (PMMA). Optik 127, 4848-4853.
5. Komagamine Y, Kanazawa M, Sasaki Y, Sato Y, Minakuchi S (2017) Prognoses of new complete dentures from the patient's denture assessment of existing dentures. Clin Oral Investig 21, 1495-1501.
6. Vojdani M, Bagheri R, Khaledi AAR (2012) Effects of aluminum oxide addition on the flexural strength, surface hardness, and roughness of heat-polymerized acrylic resin. J Dent Sci 7, 238-244.
7. Ravindranath, Sabarigirinathan C, Vinayagavel K, Rupkumar P, Sriramprabhu G, Choubey A et al. (2015) A comparative study to evaluate the mechanical properties of zirconium oxide added polymethyl methacrylate by two different methods at two different concentrations - in vitro study. Ann Int Med Dent Res 1, 161-165.
8. Yu W, Wang X, Tang Q, Guo M, Zhao J (2014) Reinforcement of denture base PMMA with ZrO_2 nanotubes. J Mech Behav Biomed Mater 32, 192-197.
9. Topouzi M, Kontonasaki E, Bikiaris D, Papadopoulou L, Paraskevopoulos KM, Koidis P (2017) Reinforcement of a PMMA resin for interim fixed prostheses with silica nanoparticles. J Mech Behav Biomed Mater 69, 213-222.
10. Vallittu PK, Lassila VP (1992) Effect of metal strengthener's surface roughness on fracture resistance of acrylic denture base material. J Oral Rehabil 19, 385-391.
11. Reyes-Acosta MA, Torres-Huerta AM, Dominguez-Crespo MA, Flores-Vela AI, Dorantes-Rosales HJ, Ramirez-Meneses E (2015) Influence of ZrO_2 nanoparticles and thermal treatment on the properties of PMMA/ZrO_2 hybrid coatings. J Alloys Compd 643, S150-158.
12. Gad M, ArRejaie AS, Abdel-Halim MS, Rahoma A (2016) The reinforcement effect of nano-zirconia on the transverse strength of repaired acrylic denture base. Int J Dent 2016, 7094056.
13. Puigdollers AR, Illas F, Pacchioni G (2016) Structure and properties of zirconia nanoparticles from density functional theory calculations. J Phys Chem C 120, 4392-4402.
14. Ayad NM, Badawi MF, Fatah AA (2008) Effect of reinforcement of high-impact acrylic resin with zirconia on some physical and mechanical properties. Rev Clín Pesq Odontol 4, 145-151.
15. Zhang XY, Zhang XJ, Huang ZL, Zhu BS, Chen RR (2014) Hybrid effects of zirconia nanoparticles with aluminum borate whiskers on mechanical properties of denture base resin PMMA. Dent Mater J 33, 141-146.
16. Al-Hiloh SA, Ismail IJ (2016) A study the effect of addition of silanized zirconium oxide nanoparticles on some properties of high-impact heat-cured acrylic resin. J Baghdad Coll Dent 28, 19-25.
17. Ahmed MA, Ebrahim MI (2014) Effect of zirconium oxide nano-fillers addition on the flexural strength, fracture toughness, and hardness of heat-polymerized acrylic resin. World J Nano Sci Eng 4, 50-57.
18. Zhou S, Garnweitner G, Niederberger M, Antonietti M (2007) Dispersion behavior of zirconia nanocrystals and their surface functionalization with vinyl group-containing ligands. Langmuir 23, 9178-9187.
19. Radford DR, Sweet SP, Challacombe SJ, Walter JD (1998) Adherence of Candida albicans to denture-base materials with different surface finishes. J Dent 26, 577-583.
20. Miettinen VM, Vallittu PK, Docent DT (1997) Water sorption and solubility of glass fiber-reinforced denture polymethyl methacrylate resin. J Prosthet Dent 77, 531-534.
21. Amin F, Iqbal S, Azizuddin S (2014) Effect of disinfectants on the colour stability of heat cure acrylic resin. J Ayub Med Coll Abbottabad 26, 530-534.
22. International Organization for Standardization (2008) Dentistry--Base polymers--Denture base polymers. ISO 20795-1:2008, Geneve.
23. Ihab N, Moudhaffar M (2011) Evaluation the effect of modified nano-fillers addition on some properties of heat cured acrylic denture base material. J Baghdad Coll Dent 23, 23-29.
24. Luo K, Zhou S, Wu L, Gu G (2008) Dispersion and functionalization of nonaqueous synthesized zirconia nanocrystals via attachment of silane coupling agents. Langmuir 24, 11497-11505.
25. Gül EB, Atala MH, Eşer B, Polat NT, Asiltürk M, Gültek A (2015) Effects of coating with different ceromers on the impact strength, transverse strength and elastic modulus of polymethyl methacrylate. Dent Mater J 34, 379-387.
26. Alla RK, Sajjan S, Alluri VR, Ginjupalli K, Upadhya N (2013) Influence of fiber reinforcement on the properties of denture base resins. JBNB 4, 91-97.
27. Lee SY, Lai YL, Hsu TS (2002) Influence of polymerization conditions on monomer elution and microhardness of autopolymerized polymethyl methacrylate resin. Eur J Oral Sci 110, 179-183.
28. Mohammed D, Mudhaffar M (2012) Effect of modified zirconium oxide nano-fillers addition on some properties of heat cured acrylic denture base material. J Baghdad Coll Dent 24, 1-7.
29. Verran J, Maryan CJ (1997) Retention of Candida albicans on

acrylic resin and silicone of different surface topography. J Prosthet Dent 77, 535-539.
30. Bollen CML, Lambrechts P, Quirynen M (1997) Comparison of surface roughness of oral hard materials to the threshold surface roughness for bacterial plaque retention: a review of the literature. Dent Mater 13, 258-269.
31. Aljafery AMA, Mah B (2015) Effect of addition ZrO_2-Al_2O_3 nanoparticles mixture on some properties and denture base adaptation of heat cured acrylic resin denture base material. J Baghdad Coll Dent 27, 15-21.
32. Al-Rifaiy MQ (2010) The effect of mechanical and chemical polishing techniques on the surface roughness of denture base acrylic resins. Saudi Dent J 22, 13-17.
33. Vuorinen AM, Dyer SR, Lassila LVJ, Vallittu PK (2008) Effect of rigid rod polymer filler on mechanical properties of poly-methyl methacrylate denture base material. Dent Mater 24, 708-713.
34. Cucci ALM, Vergani EC, Giampaolo ET, Afonso MCDSF (1998) Water sorption, solubility, and bond strength of two autopolymerizing acrylic resins and one heat-polymerizing acrylic resin. J Prosthet Dent 80, 434-438.
35. Jasim BS, Ismail IJ (2014) The effect of silanized alumina nano-fillers addition on some physical and mechanical properties of heat cured polymethyl methacrylate denture base material. J Baghdad Coll Dent 26, 18-23.
36. Arıma T, Murata H, Hamada T (1996) The effects of cross-linking agents on the water sorption and solubility characteristics of denture base resin. J Oral Rehabil 23, 476-480.
37. Zortuk M, Kılıc K, Uzun G, Ozturk A, Kesim B (2008) The effect of different fiber concentrations on the surface roughness of provisional crown and fixed partial denture resin. Eur J Dent 2, 185-190.